IRJIEST 5 (2019) 05-08
Available online at http://irjiest.com.ph
International Research Journal on Innovations in Engineering, Science and Technology

Three-dimensional printing of nanoscaled organic-inorganic siloxane hybrid composites via stereolithography

Reymark D. Maalihan*, Rigoberto C. Advincula

Department of Macromolecular Engineering, Case Western University, Cleveland, OH 44106, United States

ABSTRACT

This study presents the development and successful 3D printing of nanostructured organic-inorganic siloxane hybrid composites via stereolithography (SLA). A UV-reactive and resin-soluble methacrylolsobutyl polyhedral oligomeric silsesquioxane (MPOSS) nanohybrid is employed as a compatible and functional filler to methacrylate resin (MA) via a facile direct dispersion method. Complex and high-resolution hybrid constructs are 3D printed via in-situ photopolymerization at 405 nm wavelength. Thermogravimetric, mechanical, and wettability analysis reveal different attributes of MPOSS-MA nanocomposites filled with different amounts of MPOSS. The 3D printed structures show unique thermal, physicomechanical, and surface properties that can lead to excellent potential for new applications in the field of SLA 3D printing.

Keywords: 3D printing, organic-inorganic hybrid material, nanocomposite, polyhedral oligomeric silsesquioxanes, stereolithography

1. Introduction

In recent years, the emergence of three-dimensional printing or simply 3D printing has revolutionized the fabrication of materials such as polymers, ceramics, and metals, into high-value products. This technology takes advantage of the additive approach to manufacturing, where materials are added and joined in a layer-wise fashion until a desired physical object is formed [1,2,3]. Unlike traditional subtractive manufacturing techniques, 3D printing offers more design freedom and complexities of fabricate parts, lesser amount of wastes generated from production process, and lower fabrication costs [4,5]. With its progress, 3D printing has achieved reputation in a broad spectrum of industrial and academic fields such as microfluidics, optoelectronics, aerospace, and tissue engineering [6,7].

Stereolithography (SLA) is one of the most versatile of all 3D printing techniques for polymeric materials. It involves the use of a high-powered laser, with ultraviolet (UV) or visible light source, that cures a liquid photopolymer resin in a reservoir to create the desired 3D shape [2,3]. Owing to its high accuracy and feature resolution, SLA printed parts are typically used for applications that require the sharpest details and the smoothest surface finishes, for example, in the manufacture of biomedical devices [4]. Likewise, due to the chemistry involved in the SLA process, most of the improvements in the technology focused on synthesis of resin materials for fabrication of complex constructs [8,9].

However, typical resin formulations consist of plethora of photocrosslinkable oligomers and other modifying agents which require multistep, complicated synthesis routes to tailor the thermal, mechanical, and surface properties of the resulting 3D printed material [9,10]. Thus, a simple approach of modifying the properties of the final product can be realized by merely adding a suitable additive with complementing properties with the existing resin compositions.

Typical SLA materials containing methacrylate oligomers are sometimes too brittle and too hydrophobic for certain applications that require toughness, ductility, and hydrophilicity [5,6]. However, these properties can be easily altered by incorporation of hybrid nanomaterials such as polyhedral oligomeric silsesquioxanes (POSS). POSS have attracted substantial interest as functional materials because of their excellent compatibility with most polymer matrices and unique ability to enhance the desired structural and functional properties without compromising the valuable ones [11,12]. The organic-inorganic nanostructure of POSS plays an important role in the use of POSS-based nanocomposites for a variety of applications such as organic semiconductors, energy-related materials, drug delivery, flame retardants, and coating materials, to name a few [13]. The inner inorganic siloxane (Si-O-Si) cage of individual POSS unit provides the thermal and chemical robust framework while the outer pendant (-R and -X) organic groups provide outstanding miscibility and reactivity to the polymer matrix, forming hybrid materials [14,15].

With the current demands of developing new materials for 3D printing, it is desirable to prepare hybrid resin materials that can achieve more diverse applications with improved product performance compared with currently existing, conventional formulations. Hence, this work aims to develop 3D fabricated organic-inorganic siloxane hybrid nanocomposites using a UV-curable POSS molecule via modification of commercially available SLA resin by simple direct dispersion method. This study likewise intends to show that the thermal, mechanical, and surface attributes of the 3D-printed structures can be tailored easily by adding POSS molecules to commercially available SLA material, while maintaining the rapid, high-resolution fabrication capabilities of 3D printing.

2. Materials and methods

2.1. Materials

A commercially available photopolymerizable methacrylate -based clear resin (MA, specific gravity = 1.09-1.12, viscosity = 850-900 cP @ 25°C) was purchased from Formlabs Inc. (USA) and was used as the matrix polymer for SLA printing. A commercially available methacrylolsobutyl POSS cage mixture (MPOSS, powder form, cage content ≥ 90%) was purchased from Hybrid Plastics, Inc. (USA). It is a hybrid molecule with an inorganic siloxane at the core and organic methacryl and isobutyl groups attached at the corners of the cage.

*Corresponding author
Email address: reymark.maalihan@g.batstate-u.edu.ph

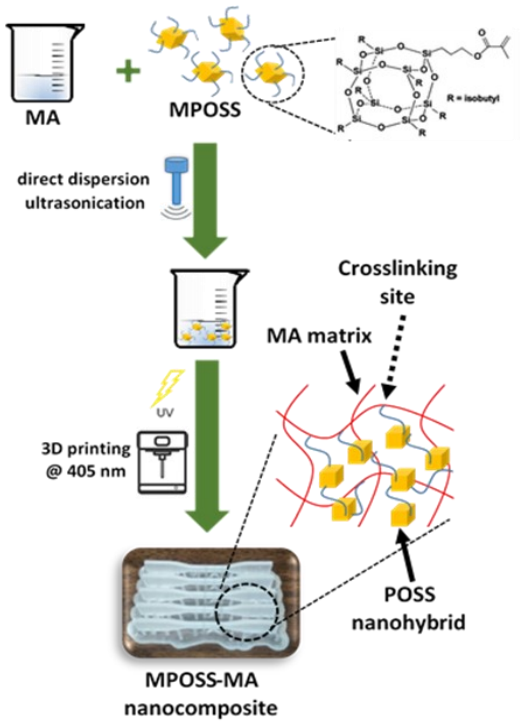

Figure 2. Preparation of 3D printed MPOSS-MA hybrid nanocomposites.

2.2 Sample preparation

The preparation of MPOSS-MA nanocomposite and SLA 3D printing process are shown in Figure 2. Based on previous studies with slight modifications [2,3], the MA-MPOSS nanocomposites containing 0, 1, 3, 5 %v/v of MPOSS were prepared by direct mixing of MPOSS with MA under mechanical stirring for 45 min, followed by ultrasonication (Cole-Parmer) under ice bath for 30 min with an amplitude of 50%, pulse duration of 5 s, and pulse interval of 5 s to ensure homogeneity before printing. Another set of 10 %v/v MPOSS resin was also prepared to check the printability of the nanocomposite at relatively higher filler loading.

A Formlabs Form 2+ SLA 3D printer was used to in-situ UV-polymerize the prepared nanocomposites and build various 3D objects. The printer is equipped with a Class 1 laser (λ = 405 nm, power = 205 mW, spot size = 140 µm) and has a build volume of 145 × 145 × 175 mm^3. A resolution (layer thickness) of 50 µm was selected for all printing operations [5].

2.3. Characterization

Changes in viscosity of the resin with increasing MPOSS loading were measured using Brookfield DV2T viscometer, at a speed of 5 rpm, multi-point averaging with points taken every 2 seconds and averaged every 10 seconds, and at temperature of 25 °C [3,8].

The dispersion of MPOSS in MA matrix was observed under Tecnai 1885 TF30 ST TEM with an accelerating voltage of 300 kV and probe current of 0.6 nA/nm spot. 3D printed MPOSS-MA films were cut into slices with a thickness of 95 nm using an ultramicrotome (Leica), placed on copper grids, and TEM images were taken. The size distribution of MPOSS was analyzed using ImageJ software [2].

The thermal stability of the nanocomposites was evaluated by thermogravimetric analysis (TGA) under nitrogen atmosphere using TA Instruments Q500 at a heating rate of 10°C/min from 25°C to 600°C. The maximum degradation temperature (T_{max}) was obtained from the first derivative (dTG) of the obtained TGA curve and the residual mass was calculated as the percentage of the mass remaining at 600°C [2,3,8].

Flexural tests under three-point bending setup were carried out using MTS universal testing machine (UTM) with a 5 kN load. Five rectangular bars for each sample with dimensions of 60.3 ± 0.04 mm x 10.4 ± 0.02 mm x 4.2 ± 0.1 mm were printed and subjected to test speed at 2 mm/min. Toughness was measured as the area under the load-displacement curve while the ductility was calculated as the percentage elongation of the sample after break in the flexural test [12].

Contact angles were measured using CAM 200 optical contact angle meter of KSV Instrument Ltd. For the contact angle measurements, ten readings were taken from each of the sample [14,15].

3. Results and discussion

3.1. Fabrication of MPOSS-MA nanocomposites: MPOSS-MA blending and SLA 3D printing

While MPOSS-resin interaction impacts the resulting properties of the nanocomposites, it may also affect the viscosity of the matrix, which is an important parameter to ensure good quality of 3D printed parts [8,12]. Thus, the influence of MPOSS on the viscosity of PMA resin was first investigated before printing the obtained formulations. As shown in Figure 3, increasing the loading of SMCS increases the viscosity of the resin as expected for filler-loaded resins. Likewise, the viscosities for resins containing up to 5% MPOSS are well below the 3000 mPa-s threshold of the 3D printer, which guarantee the printing accuracy of composites [13]. However, increasing further the MPOSS content may lead to viscosity value beyond the allowed limit, which leads to unsuccessful printing of the composites. As shown in Figure 3, uncured layers are evident for printed samples containing 10% MPOSS. If the resin is highly viscous, it prevents refilling the gap of the cured layer, resulting in complication and difficulty of the printing process [14]. Thus, only 0, 1, 3, and 5% v/v MPOSS formulations were evaluated for succeeding characterization and analysis.

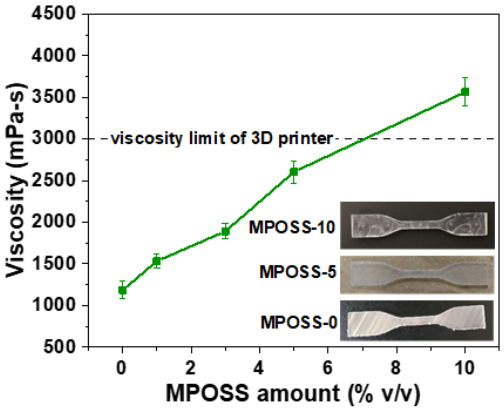

Figure 3. Viscosity of MPOSS nanocomposite resins.

TEM analysis (Figure 4) provides the morphology and dimensions of MPOSS, as well as its dispersion state in the resin matrix.

Well-dispersed, spherical shaped particles were observed in the micrographs of the representative 3D printed composites with 5% MPOSS. Multiple image analysis and Gaussian fitting of nanoparticles result in average diameter of 26.5 nm, which proves the nanoscale structure of MPOSS in the blended resin. A bar graph that shows the particle size distribution is shown in Figure 5.

To check if the addition of MPOSS affects the reproducibility of the printing process and resolution of the final product, complex structures in Figure 6 were 3D printed.

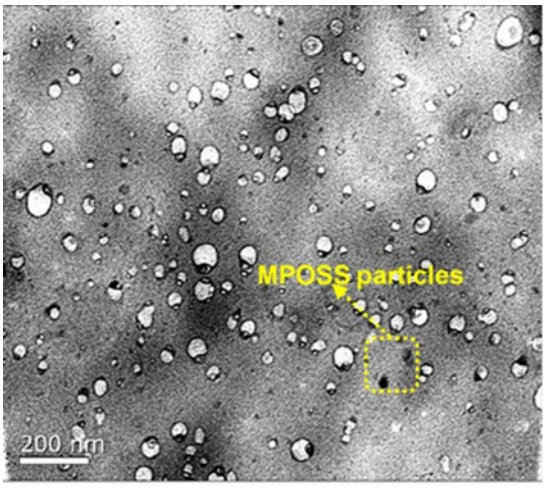

Figure 4. TEM images of 5% v/v 3D printed MPOSS-MA nanocomposites.

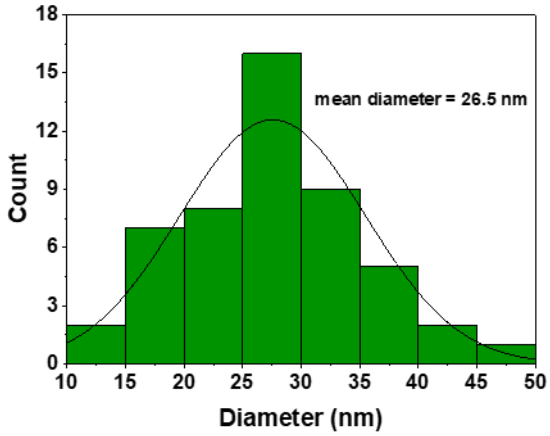

Figure 5. TEM size distribution and Gaussian fitting of monodispersed MPOSS nanoparticles.

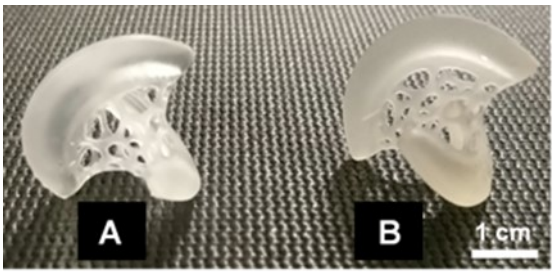

Figure 6. 3D-printed sphericon specimen for the neat (MPOSS-0) and 5 % v/v MPOSS loading (MPOSS-5).

Even at maximum printable loading of MPOSS (5 % v/ v), there is no noticeable difference in the appearance between materials printed with pure MA and MPOSS hybrid nanocomposites. It is also noted that the nanocomposites were fabricated without changing the operational settings of the 3D printer. Thus, the compatibility with current commercial 3D printers could further extend fabrication applications that demand materials with tailorable thermal, mechanical, and surface properties as discussed in the next sections.

3.2. Thermal, mechanical, and surface properties of 3D printed MPOSS-MA nanocomposite

TGA analysis was carried out to study the effect of MPOSS on the thermal stability and degradation profile of the as-prepared MPOSS-MA nanocomposites. The TGA curves of the pure MA (MPOSS-0) and MPOSS-MA nanocomposites with different loadings of MPOSS are shown in Figure 7. It is apparent in the figure that there is no significant amount of variation in terms of degradation behavior among the 3D printed specimens. This implies that different MPOSS amounts incorporated in this study do not influence the decomposition performance of the MA polymer. However, when the MA was added with MPOSS particles, the maximum degradation temperature (T_{max}) was enhanced significantly from 370.6 ± 5.6 °C to 395.7 ± 6.2 °C at 5% v/v MPOSS. Hence, the hybrid nanocomposites show good thermal stability after 3D printing. Also, increasing residual weight with amount of MPOSS at 600°C is observed, revealing the enhancement of char formation triggered by Si content of MPOSS [14].

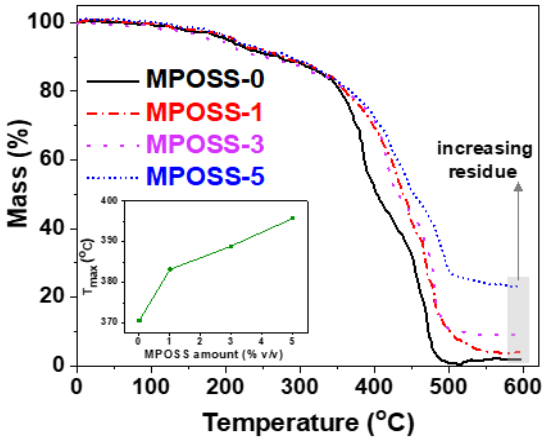

Figure 7. TGA curves of 3D printed MPOSS-MA nanocomposites. The insert illustrates the variation of maximum degradation temperature (T_{max}) with increasing MPOSS content.

Flexural tests were conducted to establish the effect of MPOSS on the mechanical properties of commercial 3D printed MA resin. The load-displacement curves of neat MA and MPOSS-MA nanocomposites are shown in Figure 8. It can be observed that the behavior is linear below 1 mm displacement, then the samples continue to retain energy until maximum strength is reached. After that, strength starts to decrease as the structure breaks. Nevertheless, the displacement increases with the amount of MPOSS present in the nanocomposite, but without significant reduction in the strength, causing a synergistic improvement in toughness (area under load-displacement curve) and ductility (percentage elongation) of the fabricated composites.

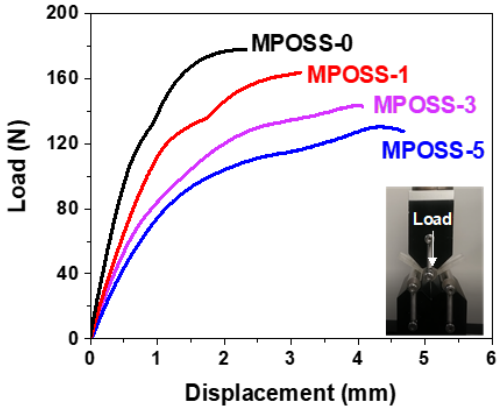

Figure 8. Flexural load-displacement curves of 3D printed MPOSS-MA nanocomposites with varying amount of MPOSS.

Results from Figure 9 shows an increase in toughness of 5% MPOSS composites from 650.5 ± 69.4 mJ (neat MA) to 970.6 ± 64.3 mJ, equal to 49.2% increase. At similar loading, the ductility likewise increased from 10.1 ± 1.7 % (neat) to 20.5 ± 2.0 %, corresponding to 103% enhancement. The

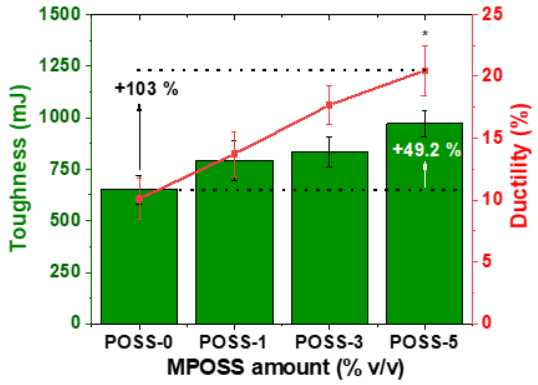

Figure 9. Toughness and ductility values of 3D printed MPOSS-MA nanocomposites with varying amount of MPOSS. *Significantly different from neat POSS (POSS-0) at $P < 0.05$.

increase in the mechanical properties can be attributed to the induced phase separation with the polymerization of the methacrylated POSS–methacrylate hybrid copolymer [14]. The toughness improvement also reduces the brittleness of the hybrid nanocomposite when exposed to elevated temperature, hence higher elongation values were attained during flexural tests [13,15].

The influence on the surface properties, specifically surface energy, of the 3D-printed material is essential for a lot of applications like in catalysis and microfluidics. As presented in Figure 10, the effect of in-situ photopolymerization on the hybrid nanocomposite network lowers the surface energy of the printed material with increasing MPOSS loading. It is therefore evident that the resulting chemical structure change in the POSS–methacrylate copolymer during 3D printing has consequently alter the surface property of the hybrid material [10,15].

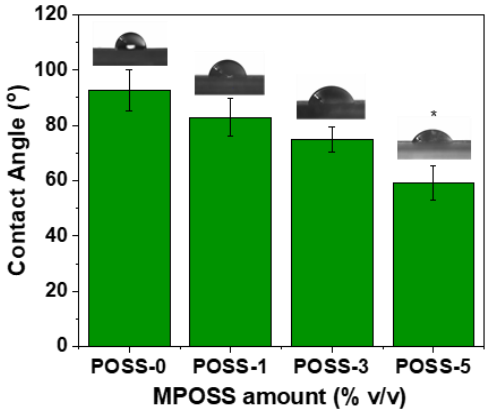

Figure 10. Wetting angle values from contact angle measurements from all specimens. *Significantly different from neat POSS (POSS-0) at $P < 0.05$.

4. Conclusions

Hybrid nanostructures were 3D fabricated by incorporating functionalized MPOSS with reactive methacryl and matrix-compatible isobutyl groups into the MA polymeric resin and exposing formulations with UV light in stereolithography (SLA) printing system. The generation of crosslinked MPOSS network in the new hybrid material resulted in numerous changes in the material properties such as an increase in maximum degradation temperature, an increase in toughness and ductility, and a decrease in surface energy. In addition, preparation and 3D printing of MPOSS hybrid nanocomposites with tailorable properties have been demonstrated, without unfavourable effect to the inherent printability of standard and existing formulations when MPOSS is directly added to the resin system.

References

[1] A. C. De Leon, Q. Chen, N. B. Palaganas, J. O. Palaganas, J. Manapat, and R. C. Advincula, "High performance polymer nanocomposites for additive manufacturing applications," *React. Funct. Polym.*, 103, 141–155, 2016.

[2] R. He, W. Liu, Z. Wu, D. An, M. Huang, H. Wu, Q. Jiang, Ji, S. Wu, and Z. Xie, "Fabrication of complex-shaped zirconia ceramic parts via a DLP-stereolithography-based 3D printing method," Ceram. Int., 44, 3, 3412-3416, 2017.

[3] Reyamark E. Zanchetta, M. Cattaldo, G. Franchin, M. Shwentenwien, J. Homa, G. Brusatin, and P. Colombo, "Stereolithography of SiOC Ceremic Microcomponents," Adv. Mater., 28, 370-376, 2016.

[4] J. Z. Manapat, Q. Chen, P. Ye, and R. C. Advincula, "3D printing of polymer nanocomposites via stereolithography," *Macromol. Mater. Eng.*, 302(9), 1–13, 2017.

[5] J. Palaganas, A. C. de Leon, J. Mangadlao, N. Palaganas, A. Mael, Y. J. Lee, H. Y. Lai, amd R. C. Advincula, "Facile preparation of photocurable siloxane composite for 3D printing," *Macromol. Mater. Eng.*, 302(5), 1–9, 2017.

[6] S. C Ligon, R. Liska, J. Stampfl, M. Gurr, and R. Mülhaupt, "Polymers for 3D printing and customized additive manufacturing," *Chem. Rev.*, 117, 15, 10212-10290, 2017.

[7] T. Zhao, X. Li, R. Yu, Y. Zhang, X. Yang, X. Zhao, L. Wang, and W. Huang, "Silicone–epoxy-based hybrid photopolymers for 3D printing." *Macromol. Chem. Phys.* 219 (10), 1–10, 2018.

[8] J. R. Dizon, Q. Chen, A. Valino, and R. C. Advincula, "Thermo-mechanical and swelling properties of three-dimensional-printed poly (ethylene glycol) diacrylate/silica nanocomposites." *MRS Commun.*, 9(1), 209–217, 2019.

[9] T. Chartier, A. Badev, Y. Abouliatim, P. Lebaudy, and L. Lecamp, "Stereolithography process: Influence of the rheology of silica suspensions and of the medium on polymerization kinetics - cured depth and width," *J. Eur. Ceram. Soc.,* 32 (8), 1625−1634, 2012.

[10] K. Pielichowski, J. Njuguna, B. Janowski, and J. Pielichowski, "Polyhedral oligomeric silsesquioxanes (POSS) -containing nanohybrid polymers.,." *Adv Polym Sci.*, 3189 201, 225-232, 2006.

[11] E. Suryani Abd Rashid, K. Ariffin, C. C. Kooi, and H. Md Aki, "Preparation and properties of POSS/epoxy composites for electronic packaging applications," *Mater. Des.*, 30 (1), 1–8, 2009.

[12] Z. Zhang, Q. Liang, J. Wang, and P. Ren, "Epoxy/POSS organic–inorganic hybrids:viscoelastic, mechanical properties and micromorphologies," *J Polym Compos.,* 28, 175-179, 2007.

[13] Y. Li, J. Zhong, L. Wu, Z. Weng, L. Zheng, S. Peng, and X. Zhang, "High performance POSS filled nanocomposites prepared via UV-curing based on 3D stereolithography printing," *Compos Part A-Appl S.*, 117, 276–286, 2019.

[14] Z. Jiang, Y. Cui, Y. Song, A. Li, and D. Sun, "MethacrylPhenyl POSS modified UV curing materials for three-dimensional printing," *SN Applied Sciences.*, 3164, 1:957, 2019.

[15] J.J Panpan, L. L. Wang, Y. Cai, and P. Liu, "The effects of structure of POSS on the properties of POSS/PMMA hybrid material," *Polym. Eng. Scie.*, 3 (55), 565 – 572, 2014.

Acknowledgement

The authors gratefully acknowledge the Swagelok Center for Surface Analysis of Materials, Case Western Reserve University, USA for TEM analysis.